
Effects of Antifolate Drugs on the Cellular Uptake of Radiofolates In Vitro and In Vivo

Cristina Müller¹, Matthias Brühlmeier², P. August Schubiger^{1,3}, and Roger Schibli^{1,3}

¹Center for Radiopharmaceutical Science ETH-PSI-USZ, Paul Scherrer Institute, Villigen, Switzerland; ²Department of Nuclear Medicine, Cantonal Hospital Aarau, Aarau, Switzerland; and ³Department of Chemistry and Applied Biosciences, ETH Zürich, Zürich, Switzerland

Targeting the folate receptor (α -FR) with radiolabeled folates for the noninvasive diagnosis and therapy of α -FR-overexpressing neoplastic tissue is of great interest. However, the tumor uptake of folate-based radiotracers was shown to be low compared with the high renal retention of radioactivity attributable to α -FR expression in the proximal tubule cells. In order to increase the tumor uptake of radiofolates, we wanted to stimulate α -FR expression or transport through coapplication of the antifolates methotrexate (MTX), raltitrexed (RTX), and pemetrexed (PMX).

Methods: ^{99m}Tc-picolyamine monoacetic acid folate (^{99m}Tc-PAMA-folate) was used for these studies. The in vitro experiments with antifolates were performed with α -FR-positive KB cancer cells. In vivo experiments were performed with KB tumor-bearing athymic nude mice. In vivo images were acquired with a small-animal SPECT/CT scanner. **Results:** KB cells incubated with solutions (10 μ mol/L) of MTX, RTX, or PMX for 24 h displayed twice as much ^{99m}Tc-PAMA-folate uptake as untreated cells. In contrast, KB tumor-bearing mice that received MTX intravenously 24 h before ^{99m}Tc-PAMA-folate showed significantly lower uptake of the radiofolate in tumors (1.35 ± 0.33 percentage injected dose per gram of tissue [%ID/g] [mean \pm SD]) and the α -FR-positive kidneys (9.35 ± 1.73 %ID/g) than did control mice (2.33 ± 0.36 and 18.48 ± 0.72 %ID/g, respectively, at 4 h after injection). When the antifolate PMX and ^{99m}Tc-PAMA-folate were injected 1 h apart, the tumor uptake of the radiotracer was unaffected (2.21 ± 0.34 %ID/g at 4 h after injection), whereas radioactivity in the kidneys was significantly decreased (1.14 ± 0.18 %ID/g at 4 h after injection). In vivo SPECT/CT studies demonstrated the specific accumulation of ^{99m}Tc-PAMA-folate in tumors and almost a complete absence of radioactivity in the renal tissue of mice preinjected with PMX.

Conclusion: Our data suggest that the preadministration of antifolates improves tumor-to-kidney ratios of radiofolates and opens a "therapeutic window" for folates radiolabeled with particle-emitting nuclides, which could otherwise be nephrotoxic.

Key Words: folate receptor; antifolate; radiopharmaceutical; ^{99m}Tc

J Nucl Med 2006; 47:2057–2064

Folic acid (FA) enters mammalian cells either through the ubiquitously distributed reduced folate carrier or through endocytosis facilitated by the folate receptor (α -FR), a high-affinity membrane-anchored protein (1). The α -FR is overexpressed on a wide variety of human tumors, including ovarian, endometrial, breast, lung, renal, and colon tumors. The highest frequency of α -FR overexpression (>90%) has been found in ovarian carcinomas (2,3). The tumor-related expression of the α -FR has led to the exploitation of FA as a molecular "Trojan horse" for the specific delivery of diagnostic or cytotoxic probes into cancer cells (4–8). Therefore, folate derivatives that are labeled with an appropriate radionuclide (for example, with ^{99m}Tc; half life of 6 h, 140 keV of γ -radiation) are suited for specific and noninvasive tumor detection with a high sensitivity. Recently, phase I and II clinical studies were completed with a radiolabeled folate derivative for the noninvasive detection of α -FR-positive renal cell and ovarian carcinomas (9,10). In this context, our group recently published a preclinical evaluation of a series of novel organometallic ^{99m}Tc-labeled radiotracers for α -FR-positive tumor targeting (11,12).

In normal tissue, the α -FR is expressed in only a few organs, which are involved in the retention and concentration of the vitamin, for example, the kidneys, choroid plexus, lungs, and placenta. Filtration of folates in the renal glomeruli and reabsorption from the primary urine via the α -FR in proximal tubules lead to an undesirably high retention of radiofolates in renal tissue (9,12,13). Because of this high accumulation of radioactivity in the kidneys, until now targeted tumor therapy with radiofolates labeled with particle-emitting isotopes could not be envisaged because of the potential nephrotoxicity.

A peculiarity of low-molecular-weight radiopharmaceuticals such as radiofolates is their fast clearance from the bloodstream. In principle, this property is desirable because high tumor-to-background ratios can be achieved shortly after tracer administration (9,13,14). On the other hand, fast clearance from the blood pool also affects tracer availability and, as a consequence, can result in low tumor accumulation. In fact, tumor uptake has been found to be low for various radiolabeled folate derivatives (12,14).

Received May 27, 2006; revision accepted Sep. 19, 2006.
For correspondence or reprints contact: Roger Schibli, PhD, Department of Chemistry and Applied Biosciences, ETH Zürich, 8093 Zürich, Switzerland.
E-mail: roger.schibli@pharma.ethz.ch
COPYRIGHT © 2006 by the Society of Nuclear Medicine, Inc.

At the beginning of these studies, we proposed that the upregulation or activation of the α -FR in neoplastic tissue would enhance the accumulation of radioactivity in α -FR-positive tumors and thus prompt an improvement in tumor-to-background ratios. On the basis of *in vitro* experiments reported in the literature, we decided to use the antifolates methotrexate (MTX), raltitrexed (RTX), and pemetrexed (PMX) to achieve this goal (15,16). Antifolates inhibit folate-dependent enzymes important for cellular purine and pyrimidine as well as amino acid metabolism. We hypothesized that cancer cells would respond to antifolate treatment and increase the expression or activation of the α -FR to cope with the “virtual” deficiency of indispensable FA. As a direct consequence, this response should lead to the enhanced accumulation of the radiolabeled folate tracer in tumor tissue.

MATERIALS AND METHODS

General

The syntheses of picolylamine monoacetic acid folate (PAMA-folate) and ^{99m}Tc -PAMA-folate (with an IsoLink kit; Tyco Healthcare) are reported elsewhere (11,12). The radiotracer ^{99m}Tc -PAMA-folate was separated from the unlabeled compound by means of high-performance liquid chromatography (HPLC). Solutions of MTX (400 $\mu\text{g}/100\ \mu\text{L}$) and leucovorin (LV; 100 $\mu\text{g}/100\ \mu\text{L}$; Fluka) were prepared with phosphate-buffered saline (PBS; 1 \times , pH 7.4) and NaCl (0.9%), respectively, followed by sterile filtration. RTX (100 $\mu\text{g}/100\ \mu\text{L}$; Tomudex; AstraZeneca AG) and PMX (400 $\mu\text{g}/100\ \mu\text{L}$; Alimta; Lilly) were diluted with sterile water and 0.9% NaCl, respectively, in accordance with the instructions of the manufacturers. The chemical structures of the compounds used for these studies are depicted in Figure 1. KB cells (CCL-17) were purchased from the American Type Culture Collection. FFRPMI cell culture medium (without FA, vitamin B₁₂, and phenol red) was purchased from Cell Culture Technologies GmbH. HPLC analyses were performed with a Merck-Hitachi L-6200A system equipped with an L-3000 tunable absorption detector, a Berthold LB 508 radiometric detector, and an XTerra MS C₁₈ reversed-phase column (5 μm , 15 cm \times 4.6 mm; Waters). HPLC solvents were aqueous triethylammonium phosphate buffer (0.05 mol/L, pH 7.0) (solvent A) and methanol (solvent B). The HPLC system started with 100% solvent A followed by a linear gradient to 20% solvent A and 80% solvent B over 15 min and then 5 min of 100% solvent A at a flow rate of 1 mL/min. Radioactivity was measured with a γ -counter (Cobra II, model B 5003; Packard).

Cell Culture

KB cells (human nasopharyngeal carcinoma cell line) were continuously cultured as monolayers at 37°C in a humidified atmosphere containing 7.5% CO₂. The cells were cultured in FFRPMI medium supplemented with 10% heat-inactivated fetal calf serum (as the only source of folate), L-glutamine, and antibiotics (penicillin at 100 IU/mL, streptomycin at 100 $\mu\text{g}/\text{mL}$, and amphotericin B [Fungizone] at 0.25 $\mu\text{g}/\text{mL}$).

In Vitro Experiments

At 24 h before each experiment, the cells were used to seed 12-well plates (8 \times 10⁵ cells in 2 mL per well) containing the antifolates MTX, RTX, and PMX or the reduced folate LV at

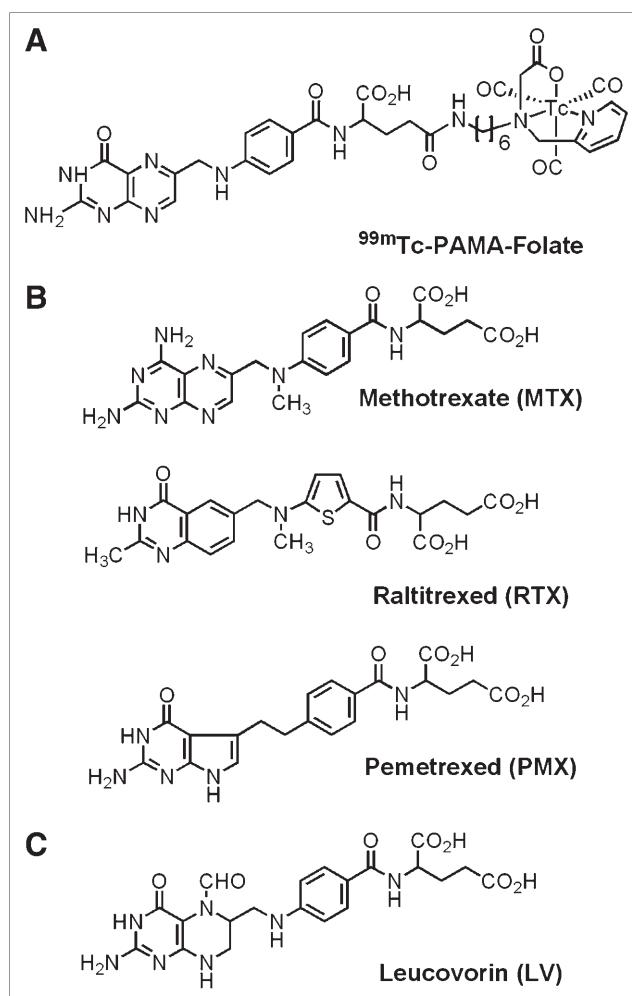


FIGURE 1. (A) Chemical structure of radiotracer ^{99m}Tc -PAMA-folate (11). (B) Chemical structures of antifolates MTX, RTX, and PMX. (C) Chemical structure of reduced folate LV.

various concentrations (0, 0.1, 1.0, and 10.0 $\mu\text{mol}/\text{L}$). The cells were then incubated at 37°C overnight to form confluent monolayers. The supernatants with the antifolates were removed from the wells, and the cell monolayers were rinsed twice with ice-cold PBS (pH 7.4). Pure FFRPMI medium (without fetal calf serum, L-glutamine, and antibiotics; 975 μL) was added to each well. The plates were preincubated at 37°C for 10 min. A solution of ^{99m}Tc -PAMA-folate (25 μL , 1 MBq/mL) was added, and the plates were incubated at 37°C for 1 h. The supernatants were then removed, and the monolayers were washed with ice-cold PBS. To determine the internalized fraction, the cell samples were washed with an acidic stripping buffer (aqueous solution of acetic acid at 0.1 mol/L and NaCl at 0.15 mol/L; pH 3) (17). α -FR blockade studies were performed as previously reported with the addition of FA (100 $\mu\text{mol}/\text{L}$) (12). The monolayers were lysed in 1N NaOH (1 mL) and transferred to 4-mL tubes, and radioactivity counts were obtained with a γ -counter (Table 1).

In Vivo Experiments

Four- to 5-wk-old female athymic nude mice (CD1-Foxn1/nu) were purchased from Charles River Laboratories. The mice were housed under conditions in accordance with Swiss veterinary

TABLE 1

In Vitro Cell Binding and Internalization (Percentage of Total Added Radioactivity) of Radiotracer ^{99m}Tc -PAMA-Folate in Cultured KB Cells Pretreated with MTX, RTX, PMX, and LV*

Dose	MTX		RTX		PMX		LV	
	Total binding	Internalization						
Control	31.8 ± 7.0	4.5 ± 0.9	25.7 ± 0.6	7.8 ± 0.5	34.6 ± 1.4	10.2 ± 1.2	33.1 ± 1.4	6.8 ± 0.8
0.1 μmol/L	42.1 ± 12.8	10.8 ± 0.1	35.3 ± 3.6	12.1 ± 1.0	55.1 ± 9.8	17.6 ± 1.6	34.8 ± 5.1	8.7 ± 0.7
1.0 μmol/L	68.0 ± 8.7	13.1 ± 1.3	48.5 ± 8.0	14.0 ± 1.9	66.9 ± 2.3	15.7 ± 1.0	29.8 ± 1.4	5.9 ± 0.8
10 μmol/L	77.3 ± 5.7	18.8 ± 1.8	64.5 ± 3.5	19.0 ± 2.2	78.8 ± 10.7	26.7 ± 4.7	15.8 ± 0.9	4.3 ± 0.4

**n* = 3. Data are reported as mean ± SD percentages.

regulations. The animals were fed a folate-deficient rodent diet (18). The mice were inoculated in the subcutis of the axilla with KB tumor cells (5×10^6 cells). Radiofolate biodistribution studies were performed 14 d after KB tumor cell inoculation. Antifolates and LV were administered intravenously or via supplementation of the drinking water for 3 d (MTX only). Antifolate doses were selected in accordance with the literature (MTX: 400 μg per mouse; RTX: 100 μg per mouse; PMX: 400 μg per mouse) (19–22). The addition of MTX (80 μg/mL) to the drinking water was calculated to be equal to the incorporation of approximately 400 μg of MTX per day per mouse. Single intravenous injections of MTX, RTX, and PMX were administered 24 h, 2 h, 1 h, 30 min, and 15 min before the administration of the radiotracer. Single intravenous injections of LV at a dose of 100 μg per mouse were administered 1 h before the administration of the radiotracer. The animals were sacrificed 30 min, 1 h, 4 h, and 24 h after the intravenous administration of ^{99m}Tc -PAMA-folate (100 μL, 350 kBq). The selected tissues were removed and weighed, and radioactivity counts were obtained to determine the percentage injected dose per gram of tissue (%ID/g).

SPECT Imaging Studies

Imaging experiments were performed by use of an X-SPECT system (Gamma Medica Inc.) with a single-head SPECT and CT device 24 h after the injection of ^{99m}Tc -PAMA-folate (200 μL, 450–600 MBq). The mice were then anesthetized with an isoflurane:oxygen mixture. The depth of anesthesia was monitored by measurement of the respiratory frequency. Body temperature was controlled by a rectal probe and kept at 37°C with a heated air stream. The scan time varied between 30 and 60 min. SPECT data were acquired and reconstructed with LumaGEM software (version 5.407; Gamma Medica). CT data were acquired with an X-Ray CT system (Gamma Medica) and reconstructed with Cobra software (version 4.5.1; Exxim-Computing Corporation). Fusion of SPECT data and CT data was performed with IDL Virtual Machine (version 6.0; ITT Visual Information Solutions) software.

RESULTS

In Vitro Effect of Antifolates and LV on Cellular Uptake of ^{99m}Tc -PAMA-Folate

For the in vitro experiments, KB cells were exposed to various concentrations of the antifolates MTX, RTX, and PMX and the reduced folate LV for 24 h before the addition of

^{99m}Tc -PAMA-folate. The cellular uptake of ^{99m}Tc -PAMA-folate increased with increasing doses of the antifolates (Table 1). In cell samples preincubated with the highest concentration of antifolates (10 μmol/L), 65%–80% of the total added radioactivity was specifically cell bound; 25%–35% was found cell bound in untreated control samples. The internalized fraction of the radiotracer was likewise increased in antifolate-pretreated cells (19%–27% vs. 5%–10% in the control samples). In cell samples incubated with LV at concentrations of 0.1 and 1 μmol/L, the uptake of ^{99m}Tc -PAMA-folate was comparable to that in control samples; a reduction of about 50% of total cell-bound radioactivity and internalization was found at a concentration of 10 μmol/L (Table 1).

In Vivo Effect of Antifolates and LV on Biodistribution of ^{99m}Tc -PAMA-Folate

Effect of Antifolate MTX Administered via Drinking Water. When MTX was administered via the drinking water for 3 d, only 0.71 ± 0.32 %ID/g (mean ± SD) of radioactivity was observed in the tumor; 2.33 ± 0.36 %ID/g ($P < 0.004$) was observed in untreated animals (supplemental Table 1). Lower levels of radioactivity were also found in the kidneys of treated animals (8.98 ± 2.57 %ID/g) than in those of control animals (18.48 ± 0.72 %ID/g) ($P < 0.018$). These results gave rise to tumor-to-kidney ratios of 0.08 ± 0.02 and 0.13 ± 0.02 , respectively. Accumulated radioactivity in other, FR-negative organs and tissues was not significantly altered after MTX treatment.

Intravenous Application of Antifolates MTX, RTX, and PMX. When the antifolate MTX was injected intravenously 24 h before ^{99m}Tc -PAMA-folate, tumor uptake was significantly reduced (1.35 ± 0.33 %ID/g at 4 h after injection of ^{99m}Tc -PAMA-folate; $P < 0.026$) (Fig. 2). The reduction in the tumor uptake of the radiotracer was accompanied by a lower accumulation of radioactivity in the kidneys (9.35 ± 1.73 %ID/g). The administration of MTX, RTX, and PMX 2 h, 1 h, 30 min, and 15 min before the injection of ^{99m}Tc -PAMA-folate revealed interesting differences among the antifolates (Fig. 2). The timing of antifolate preinjection

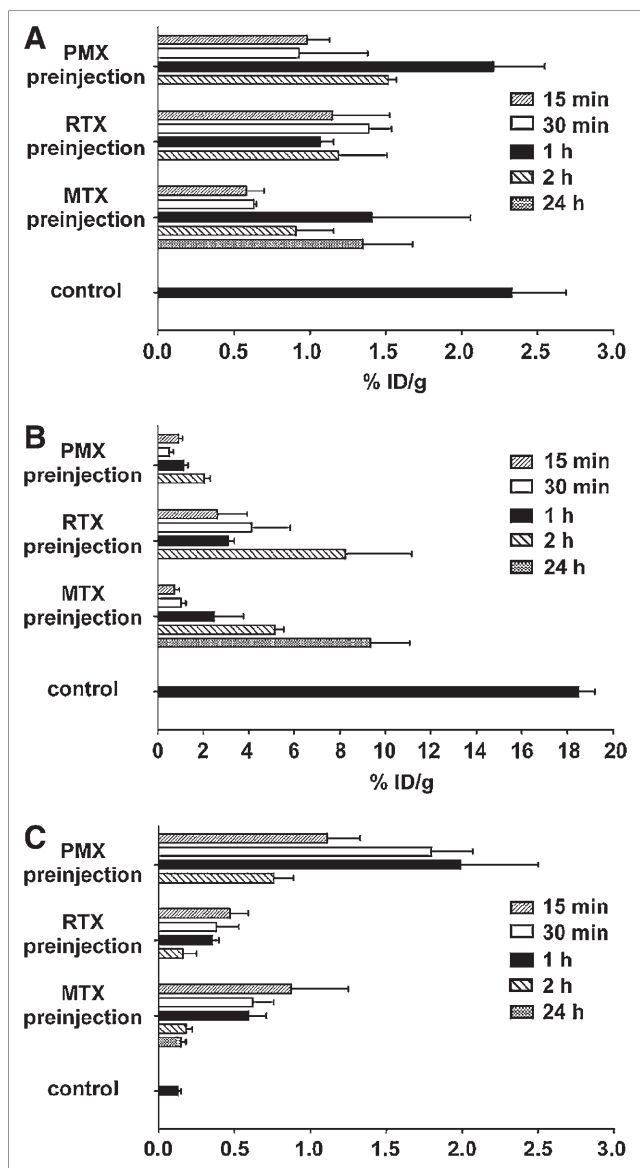


FIGURE 2. Radioactivity (%ID/g) in tumor (A) and kidneys (B) and tumor-to-kidney ratios (C) as function of time of preadministration of MTX, RTX, and PMX. (Detailed data are given in supplemental material.)

proved to be critical for sustaining the tumor uptake of the radiotracer. A 1-h preinjection of PMX resulted in almost identical amounts of radioactivity in the tumor tissue in these mice (2.21 ± 0.34 %ID/g at 4 h after injection) and in control mice (2.33 ± 0.36 %ID/g at 4 h after injection), whereas with MTX, only 0.79 ± 0.16 %ID/g was found in the tumor tissue under these conditions (Table 2). With RTX, we found the lowest reduction of tumor uptake with a 30-min preinjection (1.39 ± 0.15 %ID/g at 4 h after injection). With all tested antifolates, the decrease in accumulated radioactivity in the tumor tissue was more pronounced when they were preinjected 2 h or 15 min before the radiotracer, with a reduction of up to 75% (0.58 ± 0.12 %ID/g with a 15-min preinjection of MTX) compared with

that in untreated animals (Fig. 2). On the other hand, with all 3 tested antifolates, radioactivity retained in the kidneys gradually decreased when the injections were administered closer to the time of radiofolate administration. These 2 effects (reduced kidney uptake and retained tumor accumulation) gave rise to significantly increased tumor-to-kidney ratios when antifolates and ^{99m}Tc -PAMA-folate were administered 1 h apart (Fig. 2). They reached values of 1.99 ± 0.51 for PMX, 0.59 ± 0.12 for MTX, and 0.35 ± 0.05 for RTX; in all cases, these values were significantly higher than those in animals receiving the radiotracer only (tumor-to-kidney ratio of 0.13 ± 0.02 at 4 h after injection). The tumor-to-liver ratios were lower with MTX (0.57 ± 0.76) and RTX (0.89 ± 0.81) than in mice preinjected with PMX (2.38 ± 0.73) or in control mice (2.53 ± 2.13) (supplemental Table 1).

Time Dependence of Biodistribution of ^{99m}Tc -PAMA-Folate in Response to Antifolates. The time dependence of the tissue distribution of the radiotracer was investigated in animals preinjected with each of the antifolates 1 h before the radiotracer (Table 2). The clearance of ^{99m}Tc -PAMA-folate from the blood pool was fast and efficient (average, <0.04 %ID/g at 4 h after injection, with and without antifolate preinjection). Antifolate preinjection resulted in a decreased accumulation of radioactivity in the kidneys at all times after injection of the radiotracer. At 4 h after the injection of ^{99m}Tc -PAMA-folate, the radioactivity in the kidneys varied between 0.95 and 4.10 %ID/g, whereas values of >18 %ID/g were found in the kidneys of untreated animals. Optimal tumor-to-kidney ratios were obtained 4 h after the injection of ^{99m}Tc -PAMA-folate in mice receiving PMX (1.99 ± 0.51 ; value for control mice without antifolate preinjection: 0.13 ± 0.02). The tumor uptake of the radiotracer in mice preinjected with antifolates reached maximum values 4 h after injection with PMX and RTX (2.21 ± 0.34 and 1.39 ± 0.15 %ID/g, respectively) as well as in control mice (2.33 ± 0.36 %ID/g); with MTX, the highest tumor uptake was found 1 h after injection (1.34 ± 0.46 %ID/g). Hepatobiliary clearance of the radiotracer seemed to be slightly higher in animals receiving antifolates. However, values for accumulated radioactivity in the liver and the gastrointestinal tract varied markedly among individual animals and over time. Whereas tumor-to-liver ratios gradually increased in the control animals (from 0.20 ± 0.03 at 30 min after injection to 13.77 ± 1.90 at 24 h after injection), the maximum value for animals preinjected with PMX was found 4 h after injection of the radiofolate (2.38 ± 0.73). Accumulated radioactivity in all of the other organs and tissues was comparable to that in control mice (12).

Effect of Intravenously Administered LV. LV intravenously injected 1 h before the radiotracer resulted in an almost complete blockade of tumor and kidney accumulation of ^{99m}Tc -PAMA-folate (0.20 ± 0.04 %ID/g for tumor [$P < 0.009$] and 0.24 ± 0.09 %ID/g for kidney [$P < 0.001$] at 4 h after injection), whereas data for other organs and

TABLE 2

Biodistribution Data for Radiotracer ^{99m}Tc -PAMA-Folate in Athymic Nude Mice Bearing KB Cell Xenografts and Preinjected with MTX, RTX, and PMX 1 Hour Before Radiotracer Administration*

Treatment	Tissue or ratio	Mean \pm SD %ID/g at:			
		30 min after injection	1 h after injection	4 h after injection	24 h after injection
MTX [†]	Blood	0.14 \pm 0.01	0.06 \pm 0.02	0.02 \pm 0.00	>0.01
	Heart	0.15 \pm 0.03	0.09 \pm 0.05	0.02 \pm 0.01	0.03 \pm 0.01
	Lungs	0.21 \pm 0.05	0.11 \pm 0.05	0.02 \pm 0.01	0.02 \pm 0.00
	Spleen	0.06 \pm 0.01	0.15 \pm 0.23	0.01 \pm 0.01	0.01 \pm 0.00
	Kidneys	5.37 \pm 1.19	6.36 \pm 3.44	0.95 \pm 0.07	0.54 \pm 0.40
	Stomach	2.18 \pm 2.52	1.41 \pm 1.10	0.46 \pm 0.27	2.88 \pm 3.82
	Intestines	38.75 \pm 25.77	8.12 \pm 5.25	2.19 \pm 1.57	0.10 \pm 0.08
	Contents of intestines	109.20 \pm 68.16	80.71 \pm 75.28	17.15 \pm 13.44	0.19 \pm 0.50
	Liver	7.20 \pm 2.36	6.09 \pm 3.81	5.05 \pm 5.30	0.23 \pm 0.02
	Muscle	0.25 \pm 0.10	0.21 \pm 0.10	0.11 \pm 0.10	0.02 \pm 0.02
	Bone	0.13 \pm 0.04	0.19 \pm 0.14	0.01 \pm 0.01	0.02 \pm 0.02
	Tumor	1.04 \pm 0.26	1.34 \pm 0.46	0.79 \pm 0.16	1.03 \pm 0.40
	Tumor-to-blood	7.31 \pm 1.69	24.31 \pm 5.96	51.39 \pm 17.42	136.8 \pm 32.0
	Tumor-to-liver	0.15 \pm 0.03	0.25 \pm 0.08	0.57 \pm 0.76	4.52 \pm 1.50
Tumor-to-kidneys	0.19 \pm 0.01	0.23 \pm 0.08	0.83 \pm 0.11	2.33 \pm 1.03	
RTX [‡]	Blood	1.59 \pm 2.55	0.01 \pm 0.00	0.04 \pm 0.05	>0.01
	Heart	0.23 \pm 0.22	0.03 \pm 0.01	0.04 \pm 0.01	0.03 \pm 0.01
	Lungs	0.50 \pm 0.45	0.04 \pm 0.01	0.07 \pm 0.02	0.04 \pm 0.02
	Spleen	0.20 \pm 0.13	0.03 \pm 0.01	0.04 \pm 0.01	0.04 \pm 0.02
	Kidneys	5.66 \pm 1.16	3.08 \pm 0.28	4.10 \pm 1.71	2.63 \pm 1.29
	Stomach	0.55 \pm 0.10	0.06 \pm 0.03	0.40 \pm 0.42	0.11 \pm 0.06
	Intestines	8.24 \pm 3.08	1.13 \pm 1.27	1.01 \pm 0.28	0.63 \pm 0.28
	Contents of intestines	44.57 \pm 78.83	14.58 \pm 17.85	10.28 \pm 3.36	8.56 \pm 9.04
	Liver	6.86 \pm 5.58	0.47 \pm 0.36	2.70 \pm 2.14	1.53 \pm 0.37
	Muscle	0.19 \pm 0.08	0.04 \pm 0.03	0.07 \pm 0.03	0.05 \pm 0.02
	Bone	0.11 \pm 0.04	0.01 \pm 0.01	0.03 \pm 0.01	0.01 \pm 0.02
	Tumor	0.85 \pm 0.10	1.07 \pm 0.09	1.39 \pm 0.15	1.15 \pm 0.38
	Tumor-to-blood	6.32 \pm 7.10	84.52 \pm 28.27	66.88 \pm 54.12	120.77 \pm 43.10
	Tumor-to-liver	0.19 \pm 0.13	4.88 \pm 5.52	0.89 \pm 0.81	0.74 \pm 0.07
Tumor-to-kidneys	0.15 \pm 0.03	0.35 \pm 0.05	0.38 \pm 0.15	0.47 \pm 0.12	
PMX [§]	Blood	0.09 \pm 0.04	0.28 \pm 0.02	0.02 \pm 0.01	>0.01
	Heart	0.54 \pm 0.09	0.48 \pm 0.03	0.09 \pm 0.07	0.05 \pm 0.04
	Lungs	0.38 \pm 0.08	0.56 \pm 0.06	0.19 \pm 0.08	0.08 \pm 0.00
	Spleen	0.11 \pm 0.04	0.23 \pm 0.14	0.39 \pm 0.55	0.03 \pm 0.01
	Kidneys	3.84 \pm 0.72	4.19 \pm 0.53	1.14 \pm 0.18	0.90 \pm 0.10
	Stomach	1.38 \pm 1.36	1.19 \pm 0.55	5.85 \pm 9.27	0.53 \pm 0.19
	Intestines	17.77 \pm 14.60	3.99 \pm 5.47	1.34 \pm 0.20	0.15 \pm 0.04
	Contents of intestines	214.5 \pm 188.6	50.46 \pm 29.90	21.31 \pm 18.25	1.34 \pm 1.32
	Liver	6.87 \pm 2.82	17.78 \pm 3.64	0.97 \pm 0.25	1.10 \pm 0.04
	Muscle	0.56 \pm 0.15	0.61 \pm 0.07	0.97 \pm 0.25	0.11 \pm 0.02
	Bone	0.28 \pm 0.15	0.35 \pm 0.05	0.22 \pm 0.04	0.06 \pm 0.04
	Tumor	1.62 \pm 0.27	1.88 \pm 0.28	2.21 \pm 0.34	0.89 \pm 0.11
	Tumor-to-blood	20.52 \pm 5.66	6.84 \pm 1.47	82.07 \pm 4.39	38.97 \pm 2.57
	Tumor-to-liver	0.43 \pm 0.07	0.11 \pm 0.02	2.38 \pm 0.73	0.80 \pm 0.08
Tumor-to-kidneys	0.25 \pm 0.07	0.45 \pm 0.01	1.99 \pm 0.51	0.99 \pm 0.03	
Control [¶]	Blood	0.15 \pm 0.10	0.09 \pm 0.02	0.04 \pm 0.00	>0.01
	Heart	0.97 \pm 0.49	0.85 \pm 0.27	0.32 \pm 0.07	0.02 \pm 0.02
	Lungs	0.48 \pm 0.26	0.57 \pm 0.19	0.33 \pm 0.02	0.03 \pm 0.00
	Spleen	0.17 \pm 0.08	0.20 \pm 0.03	0.15 \pm 0.04	0.01 \pm 0.02
	Kidneys	9.68 \pm 3.59	14.37 \pm 1.35	18.48 \pm 0.72	6.90 \pm 0.72
	Stomach	0.88 \pm 0.60	0.31 \pm 0.06	0.63 \pm 0.33	3.70 \pm 6.37
	Intestines	13.74 \pm 11.37	1.89 \pm 0.37	1.49 \pm 0.23	0.76 \pm 1.15
	Contents of intestines	71.91 \pm 61.76	9.31 \pm 5.94	38.51 \pm 55.88	7.08 \pm 11.52
	Liver	6.76 \pm 4.20	0.89 \pm 0.31	2.37 \pm 2.85	0.10 \pm 0.02
	Muscle	0.90 \pm 0.42	1.06 \pm 0.33	0.54 \pm 0.05	0.05 \pm 0.04
	Bone	0.54 \pm 0.19	0.76 \pm 0.22	0.31 \pm 0.07	0.03 \pm 0.04
	Tumor	1.32 \pm 0.77	1.30 \pm 0.61	2.33 \pm 0.36	1.32 \pm 0.17
	Tumor-to-blood	9.32 \pm 1.53	15.82 \pm 11.29	58.0 \pm 12.2	255.4 \pm 115.4

TABLE 2
(Continued)

Treatment	Tissue or ratio	Mean \pm SD %ID/g at:			
		30 min after injection	1 h after injection	4 h after injection	24 h after injection
	Tumor-to-liver	0.20 \pm 0.03	1.60 \pm 0.81	2.53 \pm 2.13	13.77 \pm 1.90
	Tumor-to-kidneys	0.13 \pm 0.04	0.09 \pm 0.05	0.13 \pm 0.02	0.19 \pm 0.04

* $n = 3$.

†Preinjected at 400 μ g per mouse.

‡Preinjected at 100 μ g per mouse.

§Preinjected at 400 μ g per mouse.

¶From Müller et al. (12).

tissues were not significantly different from data for control mice (supplemental Table 2).

SPECT/CT Imaging Studies

SPECT/CT studies were performed 24 h after the administration of ^{99m}Tc -PAMA-folate in anesthetized, tumor-bearing mice by use of a dedicated small-animal SPECT/CT scanner (Fig. 3). At this time, the radiotracer had cleared from most of the organs and tissues, except for those expressing the α -FR. Mice received the antifolate PMX intravenously 1 h before the radiotracer (Fig. 3B) or the radiotracer only (Fig. 3A). The α -FR-positive tumor and kidneys were readily visualized in the ^{99m}Tc -PAMA-folate SPECT images of mouse A (Fig. 3A), whereas mouse B showed the expected decline in the renal accumulation of ^{99m}Tc -PAMA-folate when the antifolate was preinjected (Fig. 3B). Additional high-resolution SPECT/CT images of mice with and without injection of PMX ^{99m}Tc -PAMA-folate are presented in supplemental Figures 2 and 3.

Supplemental video 1 shows SPECT/CT projections of a mouse with PMX and ^{99m}Tc -PAMA-folate. The scans were

taken 24 h after injection of the radiotracer. A high-sensitivity, parallel-hole collimator was used. The scan duration was between 30 and 60 min.

Supplemental video 2 shows SPECT/CT projections of a mouse without PMX but ^{99m}Tc -PAMA-folate only. The scans were taken 24 h after injection of the radiotracer. A high-sensitivity, parallel-hole collimator was used. The scan duration was between 30 and 60 min.

DISCUSSION

Tumor-to-kidney ratios are generally low for all reported radiofolates because of the unfavorably high accumulation in α -FR-positive renal tissue (23,24) and the simultaneously low tumor uptake. Therefore, improvement in either respect, upregulation of tumor uptake or downregulation of kidney retention, is important, especially with regard to potential tumor therapy with FA coupled to particle-emitting radionuclides.

At the beginning of the present study, it seemed unlikely that a selective blockade of radiofolate uptake in the α -FR-positive kidneys could be achieved without a concomitant

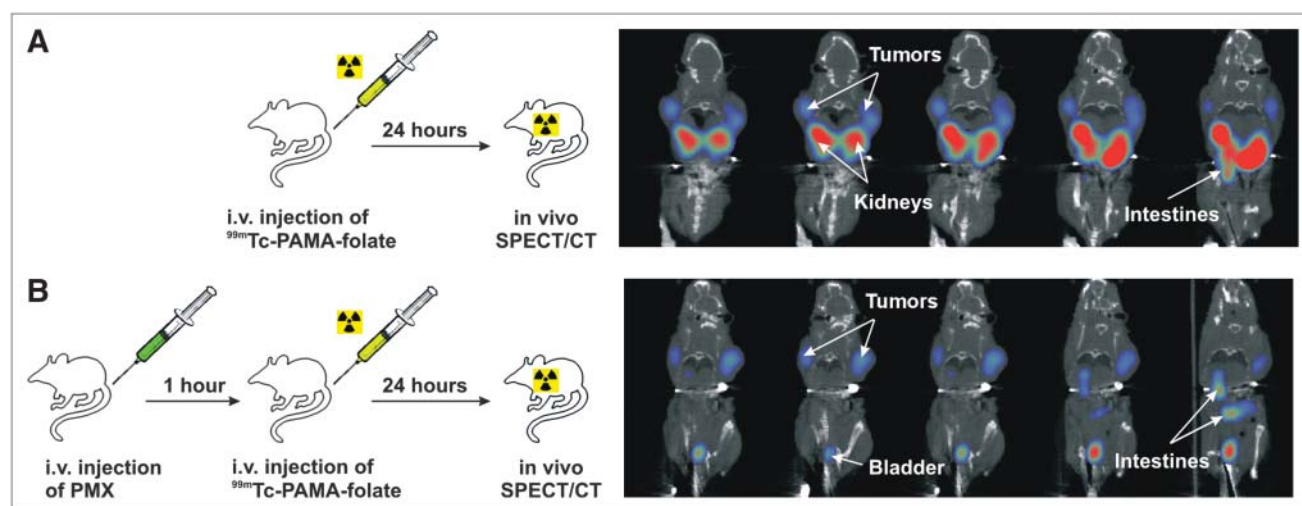


FIGURE 3. (A) Sketch of in vivo imaging procedure with ^{99m}Tc -PAMA-folate and coronal SPECT/CT sections (24 h after injection of ^{99m}Tc -PAMA-folate) at levels of tumors and kidneys of mice with subcutaneous α -FR-positive KB tumors but without PMX preinjection. (B) Procedure with PMX preinjection and corresponding coronal SPECT/CT sections. i.v. = intravenous.

inhibition of tumor uptake. Therefore, we set out to increase the tumor uptake of ^{99m}Tc -PAMA-folate through the upregulation of α -FR expression in malignant cells. α -FR expression or the activity of FR-mediated transport is regulated by extra- and intracellular folate concentrations (25,26). It was shown previously that antifolate treatment resulted in an upregulation of α -FR expression in HT-29 cancer cell cultures because of interference of the antifolates with folate metabolism (15). Thus, we speculated that antifolate pretreatment of tumor-bearing mice could also stimulate α -FR expression in vivo and enhance the tumor accumulation of ^{99m}Tc -PAMA-folate.

Our in vitro data obtained with α -FR-positive KB cells exposed to MTX, RTX, and PMX were in line with the observations reported for HT-29 cells. Preincubation of KB cells with antifolates increased the cellular uptake of the radiotracer by a factor of 2. It is noteworthy that the effect was almost identical for all antifolates, even though they target different enzymes and have different affinities for the α -FR (27,28). We also included in our studies LV, which reverses the cytotoxicity of MTX treatment at the level of dihydrofolate reductase (29). Unlike the antifolates, LV reduced the radiotracer uptake in tumor cells, a finding that is in agreement with observations published in the literature (30).

Unfortunately, our in vivo studies showed that the treatment of tumor-bearing mice with MTX administered via the drinking water or the intravenous injection of MTX at early time points (24 h) before ^{99m}Tc -PAMA-folate administration resulted in a lower accumulation of the radiotracer in the tumor tissue in these mice than in control mice. Thus, we had to revise our initial hypothesis. However, we also noted during these experiments that the kidney uptake of ^{99m}Tc -PAMA-folate was significantly reduced after antifolate treatment. Therefore, we began to investigate the biodistribution of ^{99m}Tc -PAMA-folate as a function of time after antifolate administration and made an interesting observation: when the antifolates were injected closer to the time of radiotracer administration (ideally 1 h before), a considerable reduction in radioactivity was detected in the kidneys, whereas the tumor uptake of the radiotracer was almost unaffected. This situation led to unprecedentedly high tumor-to-kidney ratios, up to 10-fold higher than those obtained in control animals (Table 2). The decreased uptake of the radiotracer in the kidneys can presumably be attributed to a saturation of the α -FR on the brush border membrane of human proximal tubule cells. This hypothesis is further supported by results published by Mathias et al., who found that the coapplication of nonradioactive deferoxamine-folate had a positive effect on the tumor-to-kidney ratio of ^{67}Ga -deferoxamine-radiofolate (31). Why RTX and PMX did not reduce the tumor uptake of ^{99m}Tc -PAMA-folate, although both antifolates are reported to bind with a high affinity to the α -FR, is the subject of current investigations. Because the time point of preinjection of the antifolates affects the kidney and tumor uptake of ^{99m}Tc -PAMA-folate, we believe that the variable pharmacokinetic profiles

of the antifolates rather than their different α -FR affinities are responsible for the observed phenomenon.

Because the preinjection of MTX, RTX, and PMX only 1 h before ^{99m}Tc -PAMA-folate administration was unlikely to stimulate α -FR upregulation in tumors (a notion supported by our in vitro experiments; supplemental Table 3), the question arose as to whether improved tumor-to-kidney ratios could also be achieved with nontoxic LV. Like MTX, LV displays a high affinity for the reduced folate carrier but binds with a significantly lower affinity to the α -FR than FA (28,30). However, we found that preinjected LV almost completely blocked both the tumor uptake and the kidney uptake of ^{99m}Tc -PAMA-folate (supplemental Table 2) as efficiently as FA (12). It is noteworthy that the preadministration of antifolates or LV exclusively affected the kidney and tumor uptake of radiofolates and had no effect on radiotracers, which do not target the α -FR (in vivo biodistribution data of ^{99m}Tc -PAMA-vitamin B₁₂ are included in the supplemental material; for the structure of ^{99m}Tc -PAMA-vitamin B₁₂, see supplemental Fig. 1).

The results of SPECT studies performed with ^{99m}Tc -PAMA-folate in tumor-bearing mice, with and without preinjection of PMX, paralleled the postmortem data. In control mice, radioactivity in the kidneys dominated the tumor accumulation; in contrast, SPECT scans revealed a virtually complete absence of radioactivity in the kidneys of mice preinjected with PMX. Radioactivity in other organs, such as the liver and lungs, was not detectable, and only residual traces of radioactivity were observed in the gastrointestinal tract 24 h after injection.

CONCLUSION

Preadministration of the antifolates MTX, RTX, and PMX selectively suppresses the uptake of ^{99m}Tc -PAMA-folate in the α -FR-positive kidneys, whereas the uptake in α -FR-positive neoplastic tissue remains almost unaltered. Our data provide strong evidence that these improvements can be achieved with any radiolabeled folate derivative when combined with an antifolate. These results open new perspectives for tumor diagnosis with radiofolates and particularly for the potential treatment of patients with cancer with a combination of antifolate chemotherapeutics and radiofolates labeled with a particle-emitting isotope.

ACKNOWLEDGMENTS

We thank Robert Waibel, Alexander Hohn, Judith Stahel, and Christine De Pasquale for technical assistance. This work was financially supported by Mallinckrodt-Tyco Inc. and Merck Eprova AG.

REFERENCES

1. Antony AC, Kane MA, Portillo RM, Elwood PC, Kolhouse JF. Studies of the role of a particulate folate-binding protein in the uptake of 5-methyltetrahydrofolate by cultured human KB cells. *J Biol Chem.* 1985;260:4911–4917.
2. Garin-Chesa P, Campbell I, Saigo PE, Lewis JL, Old LJ, Rettig WJ. Trophoblast and ovarian cancer antigen LK26: sensitivity and specificity in immunopathology

- and molecular identification as a folate-binding protein. *Am J Pathol.* 1993;142:557–567.
3. Parker N, Turk MJ, Westrick E, Lewis JD, Low PS, Leamon CP. Folate receptor expression in carcinomas and normal tissues determined by a quantitative radioligand binding assay. *Anal Biochem.* 2005;338:284–293.
 4. Leamon CP, Low PS. Folate-mediated targeting: from diagnostics to drug and gene delivery. *Drug Discov Today.* 2001;6:44–51.
 5. Russell-Jones G, McTavish K, McEwan J, Rice J, Nowotnik D. Vitamin-mediated targeting as a potential mechanism to increase drug uptake by tumours. *J Inorg Biochem.* 2004;98:1625–1633.
 6. Leamon CP, Reddy JA, Vlahov IR, et al. Synthesis and biological evaluation of EC72: a new folate-targeted chemotherapeutic. *Bioconjug Chem.* 2005;16:803–811.
 7. Gabizon A, Shmeeda H, Horowitz AT, Zalipsky S. Tumor cell targeting of liposome-entrapped drugs with phospholipid-anchored folic acid-PEG conjugates. *Adv Drug Deliv Rev.* 2004;56:1177–1192.
 8. Konda SD, Aref M, Wang S, Brechbiel M, Wiener EC. Specific targeting of folate-dendrimer MRI contrast agents to the high affinity folate receptor expressed in ovarian tumor xenografts. *MAGMA.* 2001;12:104–113.
 9. Reddy JA, Xu LC, Parker N, Vetzal M, Leamon CP. Preclinical evaluation of ^{99m}Tc-EC20 for imaging folate receptor-positive tumors. *J Nucl Med.* 2004;45:857–866.
 10. Siegel BA, Dehdashti F, Mutch DG, et al. Evaluation of ¹¹¹In-DTPA-folate as a receptor-targeted diagnostic agent for ovarian cancer: initial clinical results. *J Nucl Med.* 2003;44:700–707.
 11. Müller C, Dumas C, Hoffmann U, Schubiger PA, Schibli R. Organometallic ^{99m}Tc-technetium(I)- and Re-rhenium(I)-folate derivatives for potential use in nuclear medicine. *J Organomet Chem.* 2004;689:4712–4721.
 12. Müller C, Hohn A, Schubiger AP, Schibli R. Preclinical evaluation of novel organometallic ^{99m}Tc-folate and ^{99m}Tc-pterolate radiotracers for folate receptor-positive tumor targeting. *Eur J Nucl Med Mol Imaging.* 2006;33:1007–1016.
 13. Mathias CJ, Hubers D, Low PS, Green MA. Synthesis of [^{99m}Tc]DTPA-folate and its evaluation as a folate-receptor-targeted radiopharmaceutical. *Bioconjug Chem.* 2000;11:253–257.
 14. Trump DP, Mathias CJ, Yang ZF, Low PSW, Marmion M, Green MA. Synthesis and evaluation of ^{99m}Tc(CO)₃-DTPA-folate as a folate-receptor-targeted radiopharmaceutical. *Nucl Med Biol.* 2002;29:569–573.
 15. de Nonancourt-Didion M, Gueant JL, Adjalla C, Chery C, Hatier R, Namour F. Overexpression of folate binding protein alpha is one of the mechanism explaining the adaptation of HT29 cells to high concentration of methotrexate. *Cancer Lett.* 2001;171:139–145.
 16. Pinard MF, Jolivet J, Ratnam M, et al. Functional aspects of membrane folate receptors in human breast cancer cells with transport related resistance to methotrexate. *Cancer Chemother Pharmacol.* 1996;38:281–288.
 17. Ladino CA, Chari RVJ, Bourret LA, Kedersha NL, Goldmacher VS. Folate-maytansinoids: target-selective drugs of low molecular weight. *Int J Cancer.* 1997;73:859–864.
 18. Mathias CJ, Wang S, Lee RJ, Waters DJ, Low PS, Green MA. Tumor-selective radiopharmaceutical targeting via receptor-mediated endocytosis of gallium-67-deferoxamine-folate. *J Nucl Med.* 1996;37:1003–1008.
 19. Li Y, Looney GA, Hurwitz A. Effects of morphine on methotrexate disposition in mice. *Clin Exp Pharmacol Physiol.* 2004;31:267–270.
 20. Pritchard DM, Bower L, Potten CS, Jackman AL, Hickman JA. The importance of p53-independent apoptosis in the intestinal toxicity induced by raltitrexed (ZD1694, Tomudex): genetic differences between BALB/c and DBA/2 mice. *Clin Cancer Res.* 2000;6:4389–4395.
 21. Hughes A, Calvert P, Azzabi A, et al. Phase I clinical and pharmacokinetic study of pemetrexed and carboplatin in patients with malignant pleural mesothelioma. *J Clin Oncol.* 2002;20:3533–3544.
 22. Aherne GW, Ward E, Lawrence N, et al. Comparison of plasma and tissue levels of ZD1694 (Tomudex), a highly polyglutamatable quinazoline thymidylate synthase inhibitor, in preclinical models. *Br J Cancer.* 1998;77:221–226.
 23. McMartin KE, Morshed KM, Hazenmartin DJ, Sens DA. Folate transport and binding by cultured human proximal tubule cells. *Am J Physiol.* 1992;263:F841–F848.
 24. Sandoval RM, Kennedy MD, Low PS, Molitoris BA. Uptake and trafficking of fluorescent conjugates of folic acid in intact kidney determined using intravital two-photon microscopy. *Am J Physiol Cell Physiol.* 2004;287:C517–C526.
 25. McHugh M, Cheng YC. Demonstration of a high affinity folate binder in human cell membranes and its characterization in cultured human KB cells. *J Biol Chem.* 1979;254:1312–1318.
 26. Jansen G, Kathmann I, Rademaker BC, et al. Expression of a folate binding protein in L1210 cells grown in low folate medium. *Cancer Res.* 1989;49:1959–1963.
 27. Jackman AL, Theti DS, Gibbs DD. Antifolates targeted specifically to the folate receptor. *Adv Drug Deliv Rev.* 2004;56:1111–1125.
 28. Westerhof GR, Schornagel JH, Kathmann I, et al. Carrier- and receptor-mediated transport of folate antagonists targeting folate-dependent enzymes: correlates of molecular structure and biological activity. *Mol Pharmacol.* 1995;48:459–471.
 29. Boarman DM, Baram J, Allegra CJ. Mechanism of leucovorin reversal of methotrexate cytotoxicity in human MCF-7 breast cancer cells. *Biochem Pharmacol.* 1990;40:2651–2660.
 30. Holm J, Hansen SI, Hoier-Madsen M, Birn H, Helkjaer PE. High-affinity folate receptor in human ovary, serous ovarian adenocarcinoma, and ascites: radioligand binding mechanism, molecular size, ionic properties, hydrophobic domain, and immunoreactivity. *Arch Biochem Biophys.* 1999;366:183–191.
 31. Mathias CJ, Wang S, Low PS, Waters DJ, Green MA. Receptor-mediated targeting of ⁶⁷Ga-deferoxamine-folate to folate-receptor-positive human KB tumor xenografts. *Nucl Med Biol.* 1999;26:23–25.